# Gas Sensing Mechanism of Gold Nanoparticles Decorated Single-Walled Carbon Nanotubes

*Syed Mubeen*,[a] *Jae-Hong Lim*,[a] *Aarti Srirangarajan*,[b] *Ashok Mulchandani*,[a] *Marc A. Deshusses*,[c] *Nosang V. Myung**[a]

[a] Department of Chemical and Environmental Engineering and Center for Nanoscale Science and Engineering; University of California-Riverside; Riverside, CA 92521, USA
[b] Nanoelectronics, MIMOS Berhad, Kuala Lumpur, Malaysia
[c] Department of Civil and Environmental Engineering, Duke University, Durham, NC 27708, USA
*e-mail: myung@engr.ucr.edu

Received: June 3, 2011
Accepted: July 31, 2011

**Abstract**
Metal nanoparticles decorated single-walled carbon nanotubes (SWNTs) can lead to considerable enhancement in sensing performance towards different gas analytes, however the sensing mechanism was not clearly elucidated. The detailed sensing mechanism of hybrid gold-SWNT nanostructures toward hydrogen sulfide was investigated using field effect transistor (FET) transfer characteristics. At low $H_2S$ concentrations ($\leq 100\ ppb_V$), FET transfer characteristics show that the gold nanoparticles at the surface of SWNTs acted as nano-Schottky barriers to predominately modulate transconductance upon exposure to unfunctionalized SWNTs on gold electrodes which showed little or no response upon exposure. Although the sensitivity of Au/SWNT toward $H_2S$ was strongly dependent upon the size and number of gold nanoparticles, the sensing mechanism was independent of it.

**Keywords:** Electrodeposition, Single-walled carbon nanotube, Hydrogen sulfide, Sensors, Field effect transistors, Nanoparticles

DOI: 10.1002/elan.201100299

## 1 Introduction

Since the first demonstration of single-walled carbon nanotubes (SWNTs) as highly sensitive gas sensors [1], there have been numerous studies to understand the interaction between carbon nanotubes and gas molecules including $NH_3$, $NO_2$, CO, $H_2O$, $CH_4$, $O_2$, etc. [2–19]. The possible sensing mechanisms include electrostatic gating [1], interaction with pre-adsorbed oxygen species [3], charge transfer from adsorbed gas species to carbon nanotubes [4,5], alteration of the electrode work function which lead to change in the carrier mobility due to formation or removal of Schottky barrier [12,15,20], etc. Although significant progress has been made in understanding the sensing mechanism of pristine SWNTs towards gas molecules, the operation/sensing mode of surface modified/functionalized SWNTs still remains ambiguous [14,18,21–27]. While many covalent and noncovalent methods have been employed to functionalize SWNTs with various materials including polymers, metal oxides, and metals [25], metal nanoparticles decorated SWNTs have been extensively studied and have shown to cause great enhancement in sensing performance. Kong et al. first demonstrated that surface modification of SWNTs with palladium nanoparticles resulted in superior sensitivity toward hydrogen [26]. They attributed the response to changes in the work function of palladium nanoparticles upon exposure to hydrogen. By comparing aluminum nanoparticles decorated on SWNT to decoration on contacts, Kim et al. found that sensitivity of contact decorated devices towards $NH_3$ and $NO_2$ markedly increased compared to SWNT decorated devices, suggesting that the higher sensitivity is mainly attributed to Schottky barrier modulation between contacts/electrodes and SWNTs [27]. Kauffman et al. [24] electrochemically decorated SWNTs with different metal nanoparticles and exposed them to $NO_x$. They concluded that the sensor response is a combination of both charge transfer at the SWNT-metal nanoparticles and Schottky barrier modulation between SWNTs and electrodes and it is a function of the individual work function of metal deposited. Recently, we demonstrated that electrochemically decorated palladium and gold nanoparticles on SWNTs resulted in a 0.4% per $ppm_V$ and 0.07% per $ppb_V$ detection toward $H_2$ and $H_2S$, respectively, while carboxylated SWNTs showed no or very little response towards these analytes [18,28], again indicating that the sensing enhancement is due to the presence of metal nanoparticles. However, a number of questions remain as far as the sensing mechanism of these hybrid nanostructures is concerned. In this report, the sensing mechanism for gold nanoparticles decorated SWNTs towards very low concentrations of H2S (2–100 $ppb_V$) was systematically investigated using field effect transistor (FET) measurements at room temperature. Gold was selected as both functional metal nanoparticles and contact/electrode material for SWNTs to differentiate

  

the role of metal nanoparticles and metal contacts/electrodes on sensing mechanism. $H_2S$ was selected as analyte of interest because of its strong interaction with gold [28,29] at low concentrations ($\leq$ 100 $ppb_V$) and its absence of interaction with SWNTs [28], avoiding any interference arising from nanotube-analyte interaction.

## 2 Methods

For sensor studies, 500 μm thick heavily doped Si was used as substrate where a $SiO_2$ dielectric layer (~100 nm) was grown on the top of the substrate by thermal oxidation. Photolithography was employed for the fabrication of the source and drain gold electrodes. The thickness of gold was ~180 nm with a ~20 nm thick chromium adhesion layer. The electrode gap was approximately 3 μm. Carboxylated SWNTs (Carbon Solution, Inc. Riverside, CA, USA) dispersed in *N*,*N*-dimethylformamide solution (DMF, Sigma Aldrich, MO, USA) were dispensed between electrodes and AC dielectrophoretically aligned between the gold electrodes[30]. Note that the SWNTs in this work are on top of gold electrodes and the contact regions are fully accessible to the gas being analyzed. The aligned SWNTs were then functionalized with gold nanoparticles using electrodeposition technique.

Electrodeposition of gold nanoparticles on SWNT networks was performed using a three electrode configuration. The electrochemical cell was formed by dispensing a 3 μL drop of commercial available gold electrolyte (Techni. Inc, gold 25 ES, CA, USA) on top the SWNT networks with platinum and chlorinated Ag wires positioned inside the droplets using micropositioner. The SWNT networks along with the gold electrodes served as the working electrode, while platinum wire and chlorinated Ag wire served as the counter and pseudo-reference electrode, respectively. The electrodeposition was carried out at 25 °C and at ambient pressure. The details of electrochemical deposition are reported elsewhere [28]. After deposition, the electrodes were rinsed three times with deionized water, to remove any salt residues and other impurities present. Figure 1 shows schematic representation of a unfunctionalized SWNTs (i.e. carboxylated SWNTs) and electrochemically functionalized SWNTs, with their corresponding SEM images.

To determine the sensing mechanism, sensors were configured in FET mode by using gold electrodes as the source and drain electrodes, while heavily doped silicon substrate as the back gate electrode. 100 nm thick $SiO_2$ layer served as a dielectric layer. Transport and conductivity measurements were performed using a dual channel Keithley source meter (Keithley-Model 2636A, CA). The transfer characteristics of the device were measured by applying a constant bias of 1 V between source and drain while scanning gate voltage between ±10 V at a scan rate of 0.1 V/s. For each configuration, more than five devices were fabricated and studied to investigate the reproducibility and to ensure representativeness.

The sensors were wire-bonded and each sensor had a typical resistance of 500 KΩ to 1 MΩ at room temperature. A 3.6 $cm^3$ glass chamber with gas inlet and outlet ports for gas flow-through was placed over the sensor chip. All experiments were conducted with hydrogen sulfide gas diluted in dry air (purity: 99.998 %) at a fixed gas flow rate of 200 std. $cm^3$ $min^{-1}$. The whole sensor area was exposed to the gas being analyzed; hence any change

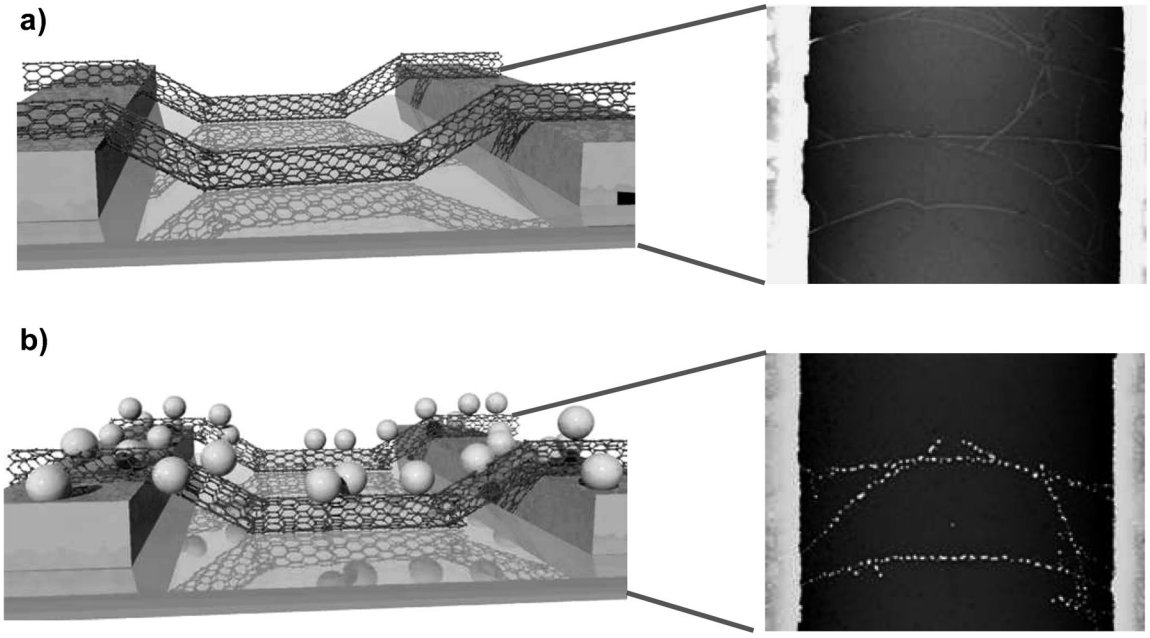


Fig. 1. Schematic representation of SWNT devices used in this study: a) Carboxylated SWNT device aligned between gold electrodes using AC field and b) Au nanoparticles decorated SWNT device. Corresponding SEM images of carboxylated and Au decorated SWNTs are also shown.

  

in device characteristics can be attributed to changes occurring along SWNT channel and across Schottky barrier between gold electrodes and SWNTs. To test the performance of SWNT-FET devices towards $H_2S$, a constant source drain voltage of 1 V was applied across the source and drain electrodes, while gate voltages were swept from −20 V to +20 V in steps of 0.5 V. In all the experiments, sensors were first exposed to zero grade dry air and then to a desired concentration of $H_2S$ gas, and then back to dry air which completed one cycle. Similar to transport measurements, for gas sensing studies, more than three devices for each sensor configuration were fabricated and studied and representative results are reported here.

## 3 Results and Discussion

Figure 2a and b shows corresponding *I–V* and FET transfer curves for SWNT-FET device, before and after electrochemical decoration with gold nanoparticles. From the *I–V* and FET transfer measurements, two clear differences are noticed. First and most obvious is the decrease of source–drain current after electrochemical decoration for all gate voltages. This is probably due to the introduction of gold nanoparticles, which are preferably deposited at defect sites on the SWNTs. These gold nanoparticles on the surface of nanotubes may form localized charge depletion regions [24] near the nanotube-nanoparticle interface resulting in charge scattering sites and thus decreasing the hole mobility. The second obvious change observed in the FET transfer characteristics is the shift in threshold voltage ($V_{th}$) towards negative gate voltage. The absolute value of the shift was found to be around 1.1 ± 0.3 V. This shift may be due to ground state charge transfer of electrons from gold nanoparticles to SWNTs resulting in electron-hole recombination and hence decreasing hole density. Another possible reason for the negative shift in $V_{th}$ may be due to the displacement of oxygen molecules [20] from the surface of SWNTs during gold nanoparticle decoration. Simplified band diagrams for carboxylated and gold decorated SWNTs are shown in the inset of Figure 2b. The electron donation from gold nanoparticles to SWNTs and/or displacement of oxygen molecules from the surface of SWNTs may cause an increase in SWNT Fermi level, resulting in greater downward band bending of valence and conduction band edges. Because of the greater downward band bending experienced by gold decorated SWNTs compared to carboxylated SWNTs, a decrease in source-drain current is observed for all gate voltages, consequently requiring more negative gate voltages for the device to switch on.

Figure 3a and 3b shows representative sensor responses for carboxylated SWNTs and gold nanoparticles decorated SWNTs FET devices towards low concentrations of $H_2S$. It can be clearly shown that at lower concentrations of $H_2S$ (10–100 $ppb_V$), the carboxylated SWNT device exhibits a negative shift in the threshold voltage ($V_{th}$) but no change in its transconductance (i.e. a measure of slope

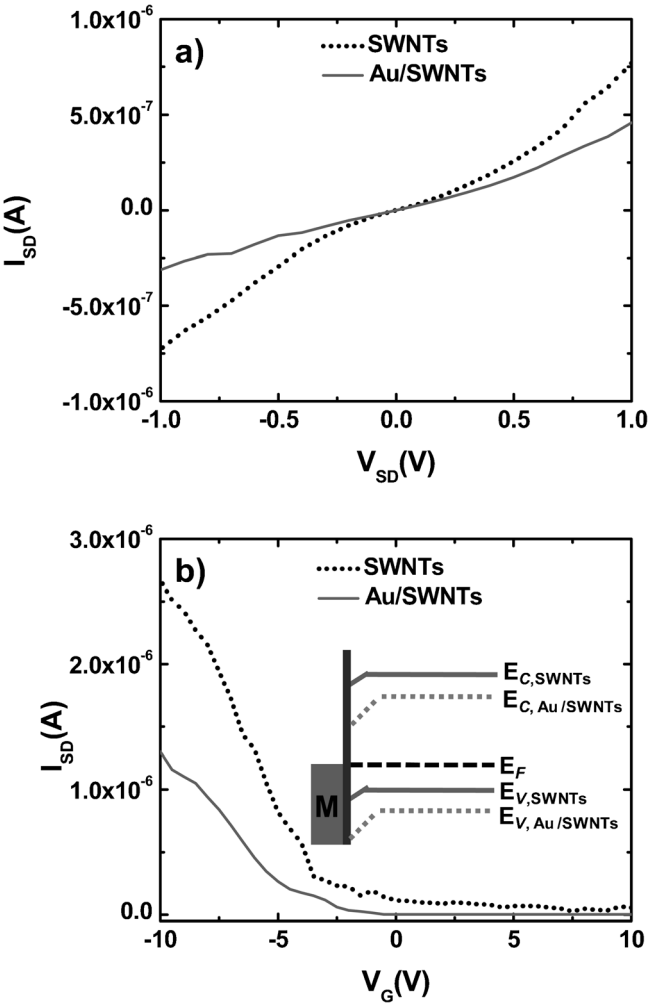


Fig. 2. a) $I_{SD}$–$V_{SD}$ curve and b) $I_{SD}$–$V_G$ (transfer characteristics) curve of SWNT FET device, before and after decoration of gold nanoparticles. The transfer curves were measured at a constant $V_{SD}$ = 1 V. Inset: Proposed band diagrams for carboxylated and gold decorated SWNT-FET device configuration. M represents the contact metal electrodes. $E_F$ is the Fermi energy level and $E_V$ and $E_C$ are the valence and conduction band energies of SWNTs and Au decorated SWNT respectively.

of source-drain current with respect to on-state gate voltage) value. If a $H_2S$ gas molecule which has high binding affinity toward gold is modifying the nanotube-gold electrode contact barrier, the result would be a change in device mobility, indicated by a "tilt" in the observed transfer curve and not the "shift" as observed here. The observed "shift" could be due to charge transfer from $H_2S$ to SWNT channel or due to the displacement of oxygen molecules from the surface of SWNTs on exposure to $H_2S$ gas. In order to corroborate the above observations, FET measurements were carried out for carboxylated SWNTs in the presence of dry air and in the presence of nitrogen (purity: 99.98%) alone (data not shown). It was observed that when the gas was shifted from dry air to nitrogen, a shift in transfer curve was observed. As theoretical studies predict very weak adsorp-

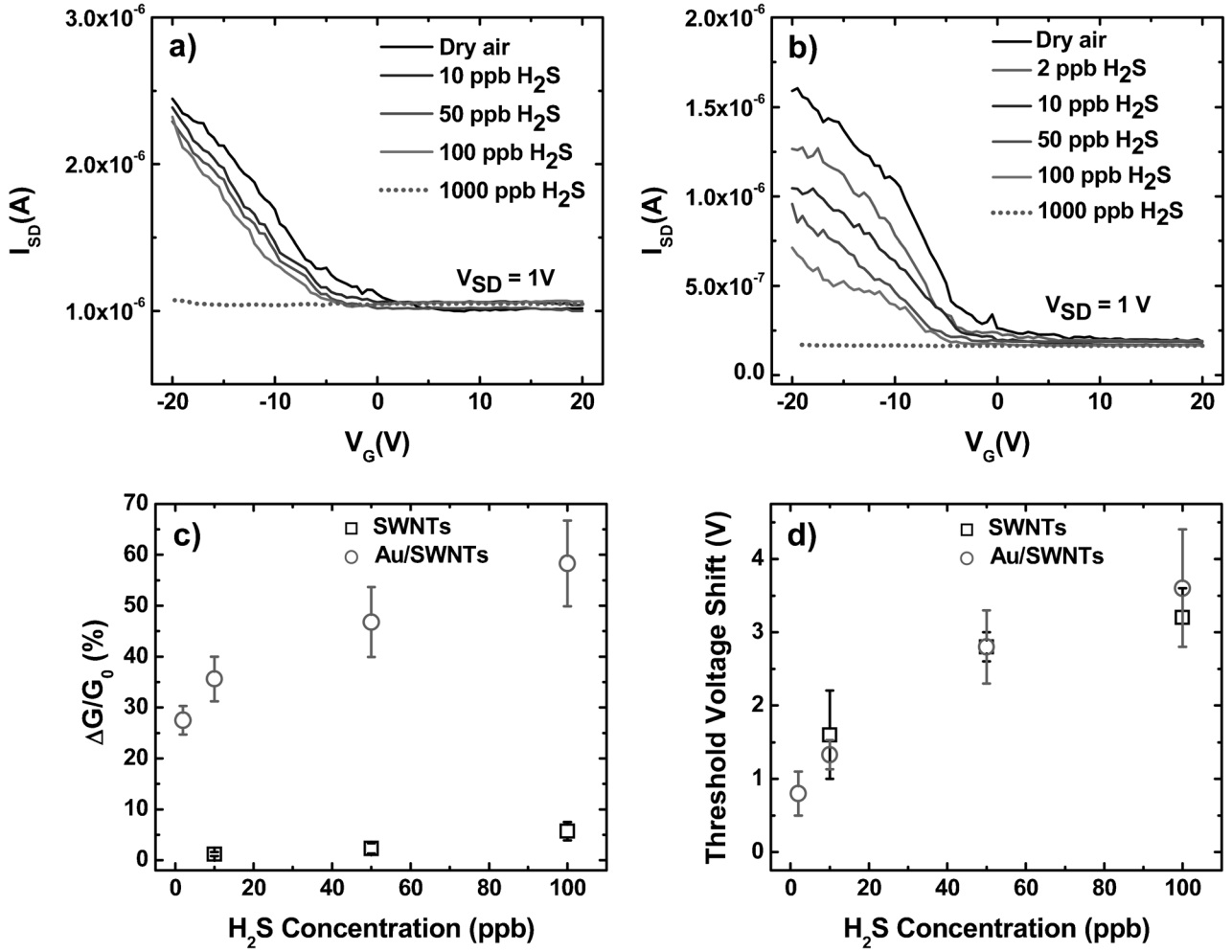


Fig. 3. Transfer characteristics of a) carboxylated SWNT-FET device and b) Au decorated SWNT-FET device before and after exposure to different concentrations of $H_2S$. All the measurements were done at 25 °C with a constant $V_{SD}$ of 1 V. c) Changes in transconductance of the device ($\Delta G/G_0$) and d) threshold voltage shift before and after exposure to $H_2S$ for carboxylated and Au/SWNT FET device. G is the slope of $I_{SD}$ with respect to $V_G$ at on-state. The error bars shown here are representation from 3 samples or more.

tion of $H_2S$ on graphitic structures at room temperature [31], and based on our above-observed results, we conclude that the observed "shift" is mainly caused by the displacement of oxygen molecules. By contrast, gold decorated SWNTs show both "shift" and "tilt" in their FET transfer curve after exposure to low concentrations (2–100 $ppb_V$) of $H_2S$. The observed shift is caused by Schottky barrier mechanism [32] where adsorbed gas molecules at metal-nanotube contact alter the work function of the metal and thereby change the band alignment resulting in carrier scattering and decreased hole mobility. Since both deposited nanoparticles and contact electrodes are gold, and no such "tilt" was observed for carboxylated SWNTs device, the "tilt" observed here is mainly due to the interaction of the gas molecule at nanoparticle–nanotube interface. Hence gold nanoparticles act as nano-Schottky barriers, whose work function is lowered locally upon exposure to $H_2S$ gas molecules, causing a decrease in source-drain current across the SWNT channel. However for high concentration of $H_2S$ (1000 $ppb_V$), both gold decorated and carboxylated SWNT-FET device showed large decrease in source-drain current with no modulation with respect to gate voltages, concluding that the modulation of Schottky barrier at nanotube-gold contact interface is the dominant mechanism for both carboxylated and gold decorated SWNT device at higher $H_2S$ concentrations. The effect of density and size of gold nanoparticles were also investigated by examining Au/SWNT hybrid nanostructures synthesized with different deposition charge. For example, higher applied deposition charge led to large gold nanoparticles decorated on SWNTs. Independent of the deposition charge, Au/SWNT show both "shift" and "tilt" in their FET transfer curve upon exposure to $H_2S$, which indicated that the sensing mechanism was independent of size and density of gold nanoparticles.

Figure 3c and 3d analyzes the changes in device transconductance ($\Delta G/G_0$) and changes in carrier concentration (threshold voltage shift) for carboxylated SWNTs and gold nanoparticles decorated SWNTs-FET devices at different concentrations of $H_2S$. A large change in trans-

  

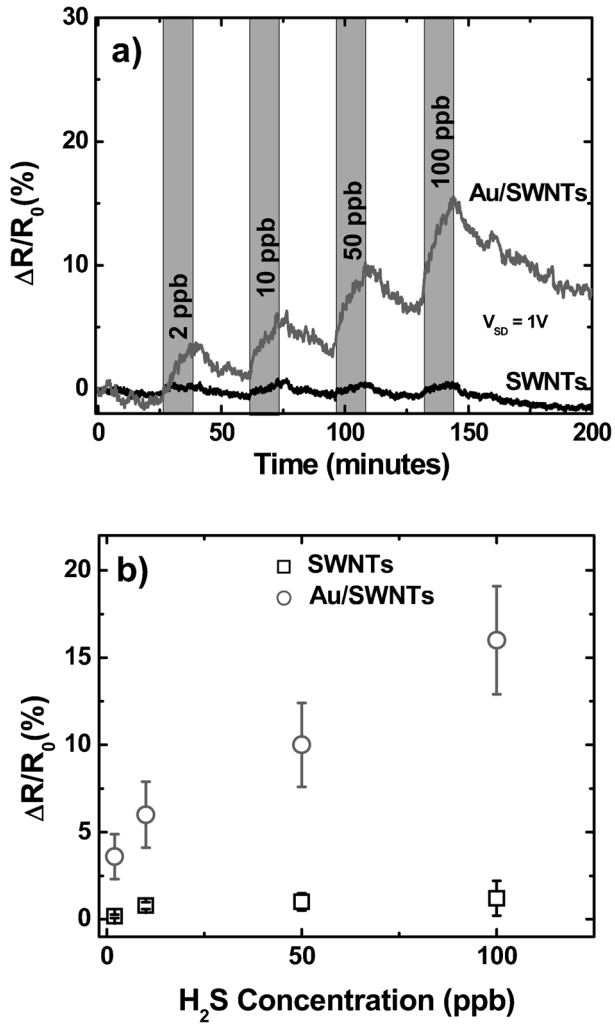


Fig. 4. a) Real time detection of $H_2S$ at 25 °C under zero gate voltage for carboxylated and gold decorated SWNT device with a constant $V_{SD}$ of 1 V. b) Calculated sensitivity ($\Delta R/R_0$) of carboxylated and Au/SWNT devices, where $R$ is the resistance of the device at $V_{SD}$ of 1 V and at zero gate voltage. The error bars shown here are representations from 3 samples or more.

conductance with increasing $H_2S$ concentrations is observed for Au-SWNTs, compared to practically no change observed in the carboxylated SWNTs device. This indicates that the sensing region that is most responsible for conductance modulation is localized near the gold nanoparticle–nanotube interface. As the absolute values of threshold voltage shift are almost similar for both carboxylated and gold decorated samples, it is hard to determine whether the shift observed in gold decorated SWNTs is because of electrostatic gating at nanotube–nanoparticle interface or displacement of oxygen molecules as observed for carboxylated SWNT device or a combination of both.

Figure 4a shows real-time responses of gold decorated and carboxylated SWNT device towards different concentrations of $H_2S$ (at zero gate voltage). The sensitivity ($\Delta R/R_0$) of Au decorated and carboxylated SWNT devices is reported in Figure 4b. The results clearly show that the gold decorated SWNT device has a lower detection limit and a greater sensitivity towards $H_2S$ compared to the carboxylated SWNT device. As was demonstrated above, this significant increase in sensitivity is primarily due to the increased nano-Schottky barriers introduced by gold decoration, resulting in local modulation of the work function upon exposure to gas molecules.

## 4 Conclusions

The sensing mechanism of carboxylated and gold decorated SWNT-FET devices towards $H_2S$ was investigated. Since the SWNTs were functionalized with same material as the electrode contacts and the SWNTs had very low adsorption capacity for the gaseous analyte, the role of the functional elements on sensing could be isolated and explained. These results indicate that gold nanoparticles functionalized on SWNT surface act as nano-Schottky barriers and play a dominant part in hole mobility modulation by gaseous molecule interaction. We speculate that the same mechanism may exist for other metals functionalized on the surface of SWNTs. Of course, the extent of conductance modulation will depend on the choice of the metallic functional element and on the gaseous analyte. A greater understanding of the role of functional elements in sensing will help in optimizing SWNT-FET devices and will results in more sensitive and selective gas sensors.

## Acknowledgements

Funding for the project was provided by the NIH Genes, Environment and Health Initiative through award U01 ES 016026 and the Fundamental R&D Program for Core Technology of Materials funded by the *Ministry of Knowledge Economy, Republic of Korea*.

## References

[1] J. Kong, N. R. Franklin, C. Zhou, M. G. Chapline, S. Peng, K. Cho, H. Dai, *Science* **2000**, *287*, 622.
[2] S. Peng, K. Cho, *Nanotechnology* **2000**, *11*, 57.
[3] P. G. Collins, K. Bradley, M. Ishigami, A. Zettl, *Science*, **2000**, *287*, 1801.
[4] H. Chang, J. D. Lee, S. M. Lee, Y. H. Lee, *Appl. Phys. Lett.* **2001**, *79*, 3863.
[5] J. Zhao, A. Buldum, J. Han, J. P. Lu, *Nanotechnology* **2002**, *13*, 195.
[6] K. Bradley, J. C. P. Gabriel, A. Star, G. Gruner, *Appl. Phys. Lett.* **2003**, *83*, 3821.
[7] K. Bradley, J. C. P. Gabriel, M. Briman, A. Star, G. Gruner, *Phys. Rev. Lett.* **2003**, *91*, 218301.
[8] T. Yamada, *Phys. Rev. B* **2004**, *69*, 125408.
[9] C. W. Bauschlicher, A. Ricca, *Phys. Rev. B* **2004**, *70*, 115409.
[10] X. Liu, Z. Luo, S. Han, T. Tang, D. Zhang, C. Zhou, *Appl. Phys. Lett.* **2005**, *86*, 243501.
[11] X. Feng, S. Irle, H. Witek, K. Morokuma, R. Vidic, E. Borguet, *J. Am. Chem. Soc.* **2005**, *127*, 10533.

  

[12] Y. T. Amada, *Appl. Phys. Lett.* **2006**, *88*, 083106.
[13] J. Zhang, A. Boyd, A. Tselev, M. Paranjape, P. Barbara, *Appl. Phys. Lett.* **2006**, *88*, 123112.
[14] A. Star, V. Joshi, S. Skarupo, D. Thomas, J. C. P. Gabriel, *J. Phys. Chem. B* **2006**, *110*, 21014.
[15] N. Peng, Q. Zhang, C. L. Chow, O. K. Tan, N. Marzari, *Nano. Lett.* **2009**, *9*, 1626.
[16] T. Zhang, M. B. Nix, B. Y. Yoo, M. A. Deshusses, N. V. Myung, *Electroanalysis* **2006**, *18*, 1153.
[17] T. Zhang, S. Mubeen, E. Bekyarova, B. Y. Yoo, R. C. Haddon, N. V. Myung, M. A. Deshusses, *Nanotechnology* **2007**, *18*, 165504.
[18] S. Mubeen, T. Zhang, B. Y. Yoo, M. A. Deshusses, N. V. Myung, *J. Phys. Chem. C* **2007**, *111*, 6321.
[19] T. Zhang, S. Mubeen, N. V. Myung, M. A. Deshusses, *Nanotechnology* **2008**, *19*, 332001.
[20] D. S. Hecht, R. J. A. Ramirez, M. Briman, E. Artukovic, K. S. Chichak, J. F. Stoddart, G. Grüner, *Nano Lett.* **2006**, *6*, 2031.
[21] Y. Fan, B. R. Goldsmith, P. J. Collins, *Nature Mater.* **2005**, *4*, 906.
[22] T. M. Day, P. R. Unwin, N. R. Wilson, J. V. Macpherson, *J. Am. Chem. Soc.* **2005**, *127*, 10639.
[23] B. M. Quinn, C. Dekker, S. G. Lemay, *J. Am. Chem. Soc.* **2005**, *127*, 6146.
[24] D. R. Kauffman, A. Star, *Nano Lett.* **2007**, *7*, 1863.
[25] J. Wang, Y. Lin, *Trends Anal. Chem.* **2008**, *27*, 619.
[26] J. Kong, M. G. Chapline, H. Dai, *Adv. Mater.* **2001**, *13*, 1384.
[27] B. K. Kim, N. Park, P. S. Na, H. M. So, J. J. Kim, H. Kim, K. J. Kong, H. Chang, B. H. Ryu, Y. Choi, J. O. Lee, *Nanotechnology* **2006**, *17*, 496.
[28] S. Mubeen, T. Zhang, N. Charutraprayoon, Y. Rheem, A. Mulchandani, N. V. Myung, M. A. Deshusses, *Anal. Chem.* **2010**, *82*, 250.
[29] J. Geng, M. D. R. Thomas, D. S. Shephard, B. F. G. Johnson, *Chem. Commun.* **2005**, 1895.
[30] S. Baik, M. Usrey, L. Rotkina, M. Strano, *J. Phys. Chem. B* **2004**, *108*, 15560.
[31] W. Michalak, E. Broitman, M. A. Alvin, A. J. Gellman, J. B. Miller, *Appl. Catal. A* **2009**, *362*, 8.
[32] I. Heller, A. M. Janssens, J. Mannik, E. D. Minot, S. G. Lemay, C. Dekker, *Nano Lett.* **2008**, *8*, 591.

  